

CHAPTER 5

RESULTS AND DISCUSSIONS

In this chapter, we will present the results of CVD parameters to diamond films. First, the results of deposition time to CVD diamond growth is discussed. Then, the effect of methane concentrations to the films morphology, and films qualities will be presented. In addition, the effect of laser used in Raman spectrum will be presented. In the last section, the effect of CH_4 concentration and deposition pressure to the films morphology, and films qualities will be presented.

5.1 Effect of Time Dependence on Film Morphology

Fig. 5.1a-d shows the SEM images of the CVD diamond films at different deposition times. At deposition time of 1 hour (Fig. 5.1a), film contains a very small individual diamond nuclei, which is confirmed by Raman result showed in Fig. 5.3. With increase deposition time to 5 hours (Fig. 5.1b), the diameter of individual diamond nuclei is increased. At the deposition time of 10 hours (Fig. 5.1c), the diamond crystalline shows slightly facet phase with the grains diameter about $0.5 \mu\text{m}$. At the deposition time of 18 hour (Fig. 5.1d), the diamond crystalline density increased to cover the entire substrate. The clear facets and edges can be found, as showed in Fig. 5.2.

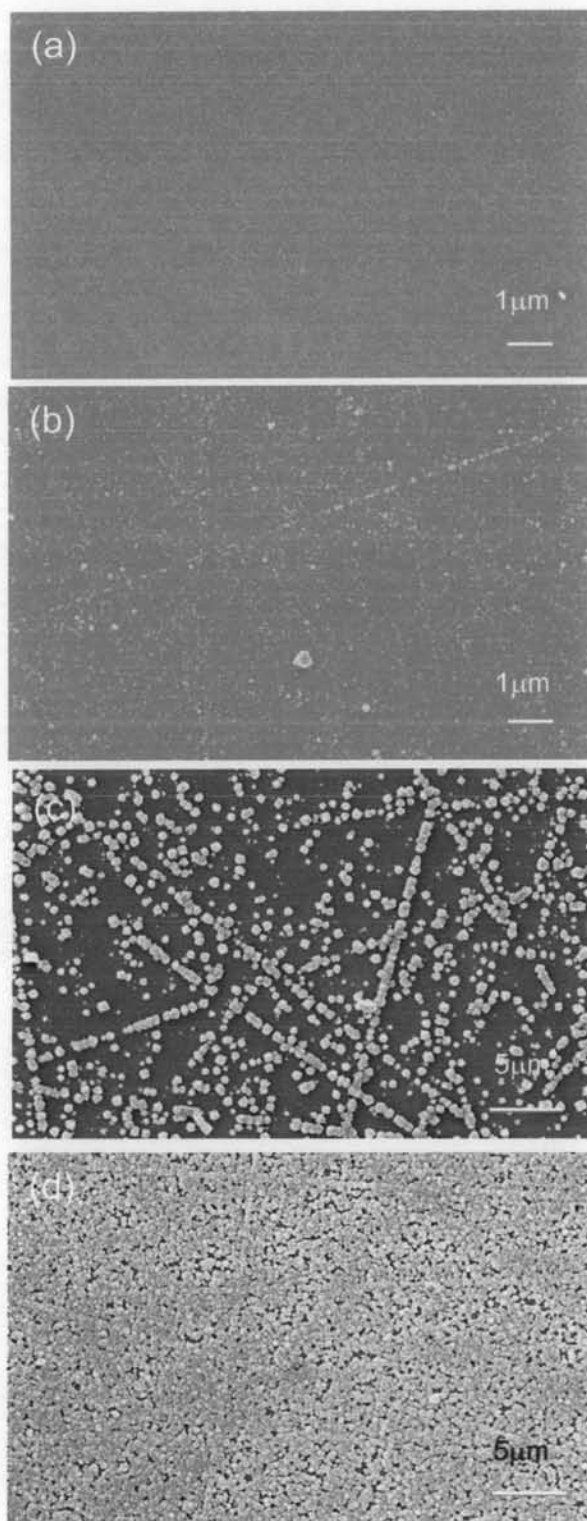


Figure 5.1: SEM images of CVD diamond films at different deposition times under CH_4 concentration of 1%, deposition pressure of 30 Torr, and microwave power of 450 watt at deposition time of 1 hour (a), 5 hour (b), 10 hour (c), and 18 hour (d), respectively.

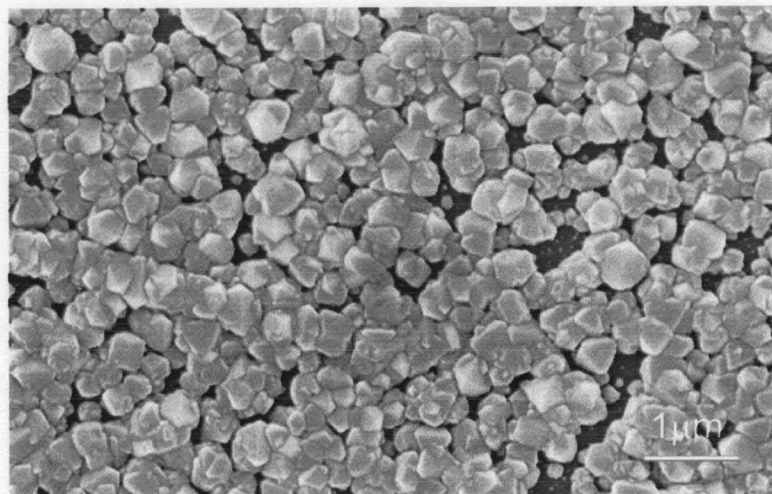


Figure 5.2: SEM image of polycrystalline film at deposition time of 18 hours with the magnification of 15000.

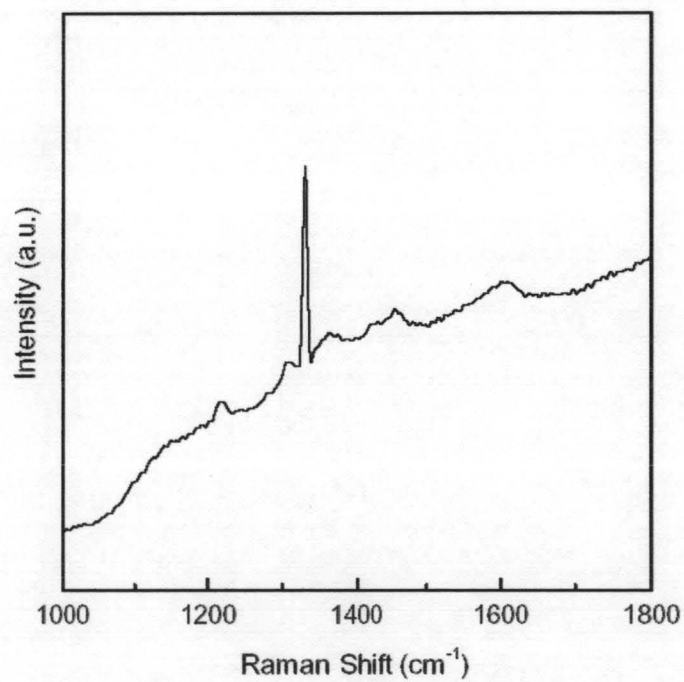


Figure 5.3: Raman spectrum of film at deposition time of 1 hour, the sharp peak at 1332 cm^{-1} confirm that the substrate is covered with diamond nuclei.

5.2 Effect of Seeding methods on Films Morphologies

The surface pretreatment methods can enhance the nucleation density of diamond as already mentioned in section 2.3.3. The effects of two different methods of surface pretreatment, ultrasonic agitation and hand scratching, on the obtained CVD diamond films are studied. In the ultrasonic scratching, Si substrate is rinsed with detergent, shaken in ultrasonic basin filled with the mixture of $1\mu\text{m}$ diamond powder and methanol (0.240/9.50) for 6 hours, then ultrasonically cleaned again for 30 mins each in ethanol, methanol, and deionized water, respectively. Finally, Si substrate is dried with a nitrogen blowgun. Fig. 5.4 shows SEM images of CVD diamond films prepared by; (a) hand scratching, and (b) ultrasonic scratching methods. It is clearly seen that the film surface prepared by hand scratching yield preferable higher nucleation density than film prepared by ultrasonic scratching method. This could be the result from a number of the groove which occur from the hand scratching. A number of the groove on substrate surface also contribute to reduce the diffusion of atom and molecule that deposit on surface during growth processes. In this work, we choose hand scratching for substrate preparation. Fig. 5.5 shows AFM images of Si substrate prepared by ultrasonic and hand scratching.

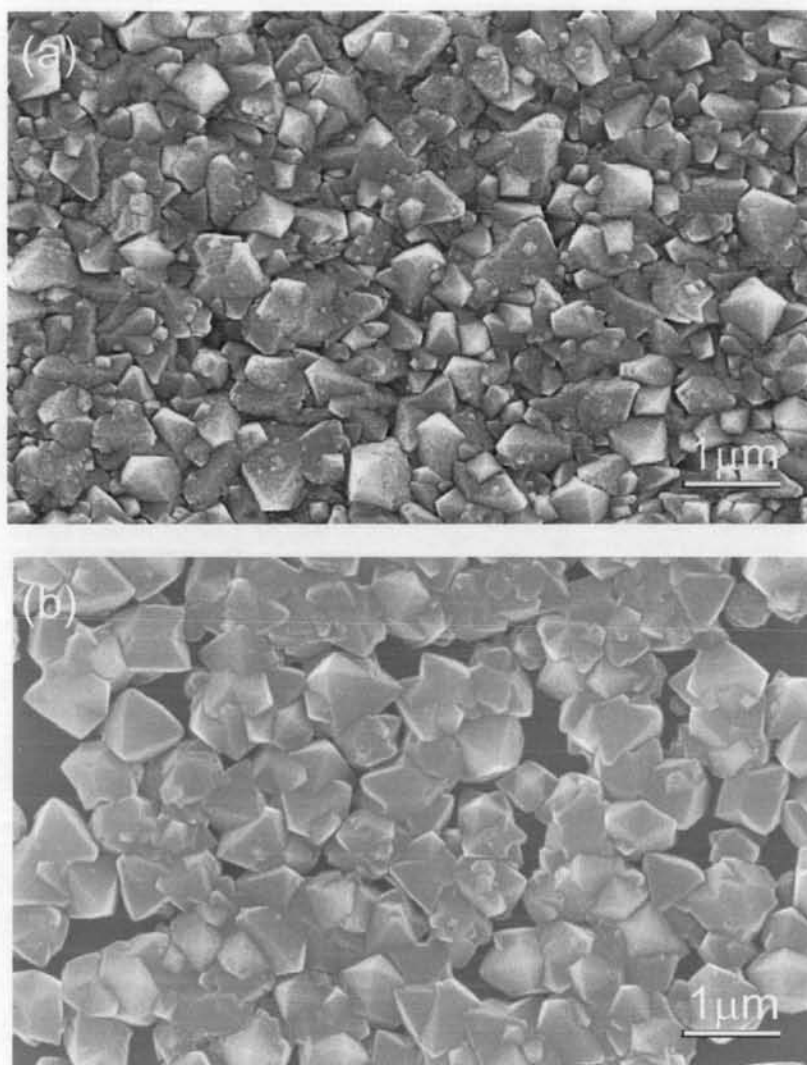


Figure 5.4: SEM photographs show surface morphologies of CVD diamond films; (a) prepared by hand scratching, and (b) prepared by ultrasonic scratching, respectively. Both film were grown under the CH_4 concentration of 1%, deposition pressure of 30 Torr, and microwave power of 450 watt.

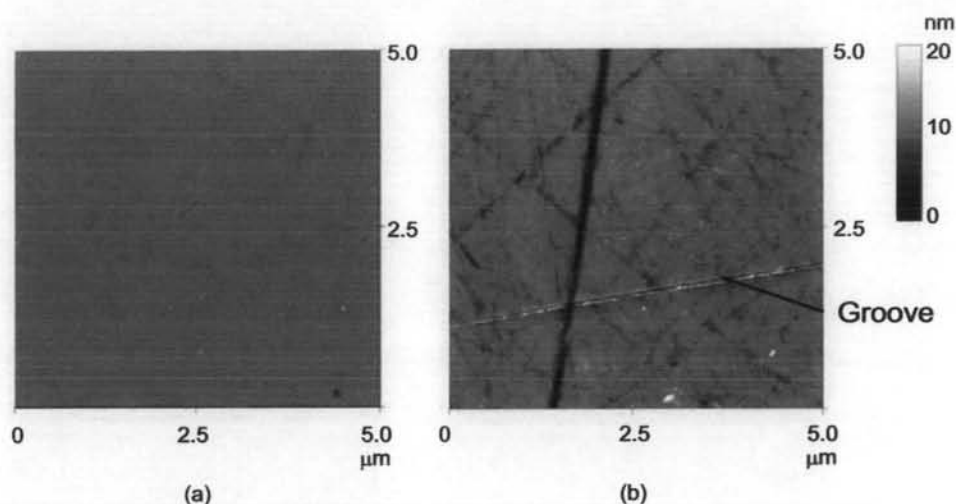


Figure 5.5: 2D AFM images ($5 \times 5 \mu\text{m}^2$) of Si substrate prepared by (a) ultrasonic scratching, and (b) hand scratching, respectively.

5.3 Effect of CH_4/H_2 Gas Mixtures on Diamond Films

The CVD diamond films were deposited under the variation of CH_4 in H_2 gas mixtures, as showed in Table 5.1.

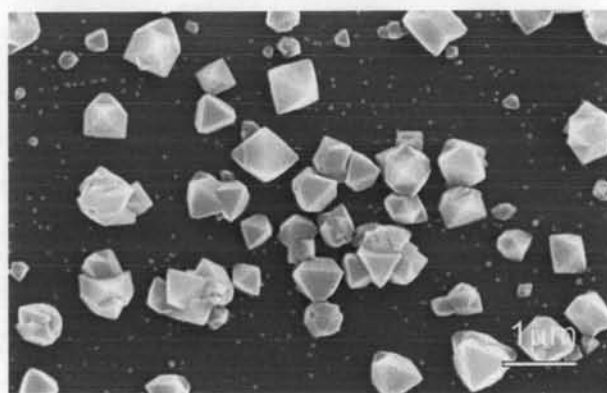
Table 5.1: The flow rate ration of CH_4 to H_2 for CVD diamond film samples.

Sample	VF1	VF2	VF3	VF4	VF5
$\text{CH}_4:\text{H}_2(\text{sccm}:\text{sccm})$	0.5:100	1:100	2:100	3:100	5:100

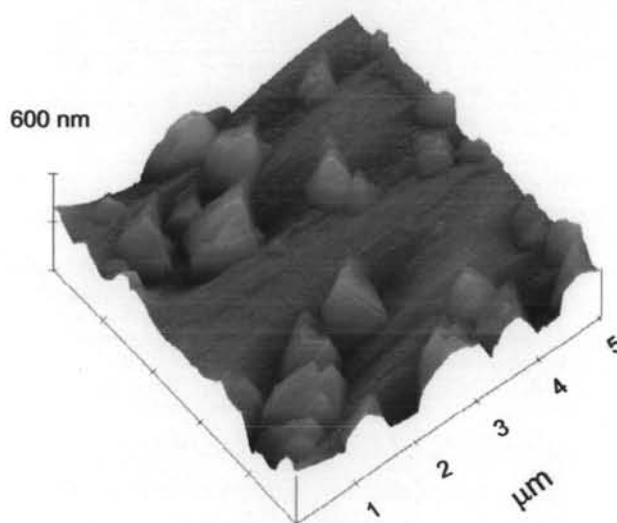
Films VF1-VF5 were grown under the deposition pressure of 30 Torr, the microwave power of 450 watt, the substrate temperature of 430-470°C, and deposition time of 30 hour. The effect of CH_4 concentrations on surface morphology, surface roughness as well as the type of bonding in these films will be presented and discussed in the following.

5.3.1 Films morphology and roughness

The surface morphology of CVD diamond films taken with SEM and AFM at the CH_4 concentrations between 0.5-5% are showed in Fig. 5.6-5.10. With increasing CH_4 concentrations, film surface morphology changes from scatter well-faceted to non-faceted continuous films.

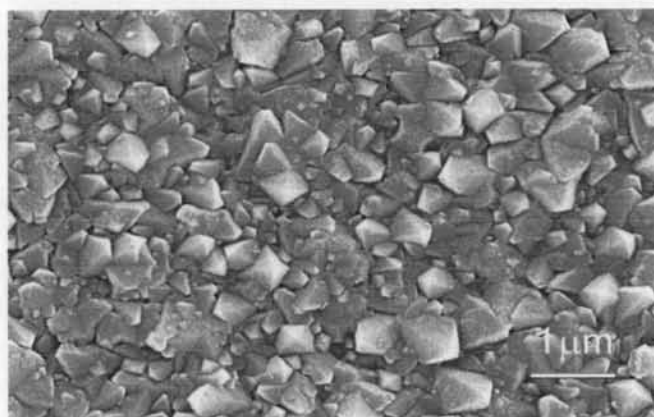


(a)

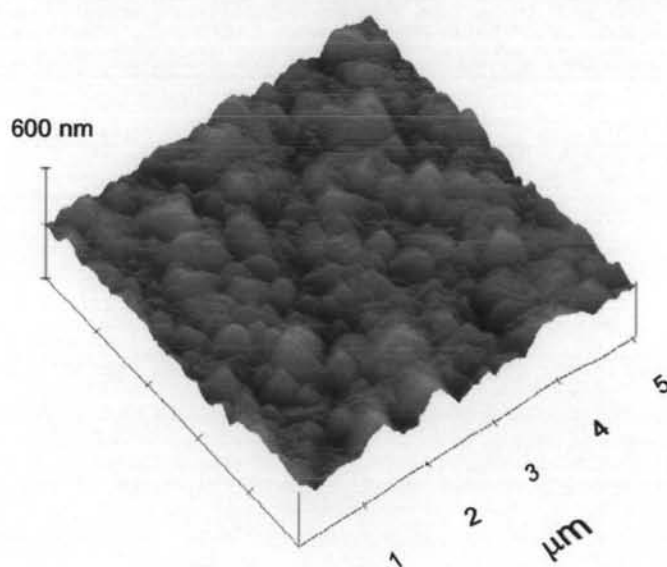


(b)

Figure 5.6: (a) SEM photograph, and (b) 3D AFM image of sample VF1, which was grown under the CH_4 of 0.5%, deposition pressure of 30 Torr.



(a)



(b)

Figure 5.7: (a) SEM photograph, and (b) 3D AFM image of sample VF2, which was grown under the CH_4 of 1.0%, deposition pressure of 30 Torr.

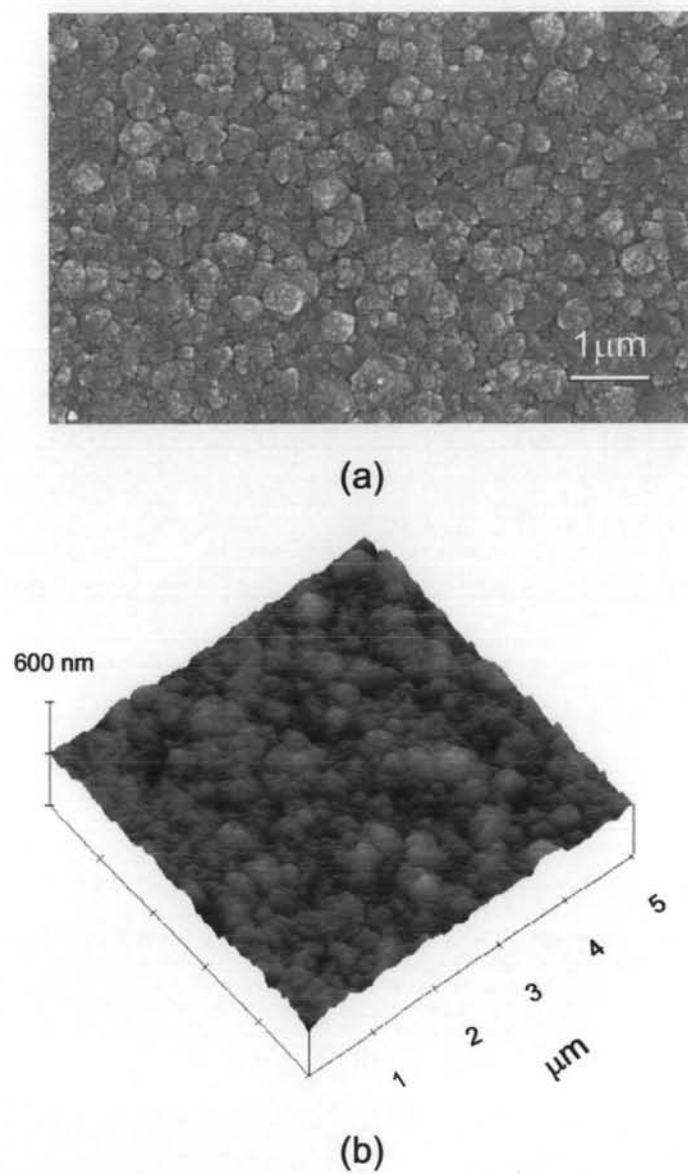
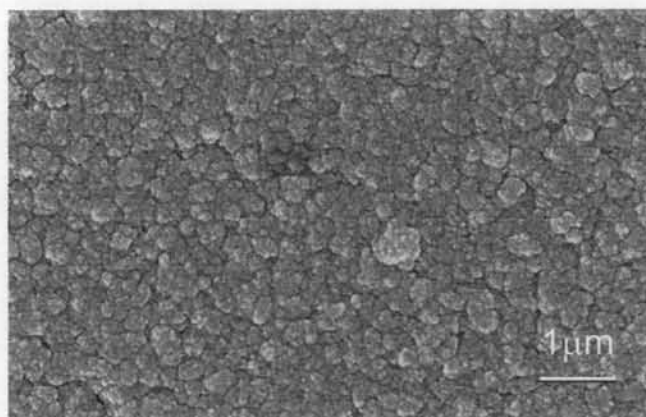
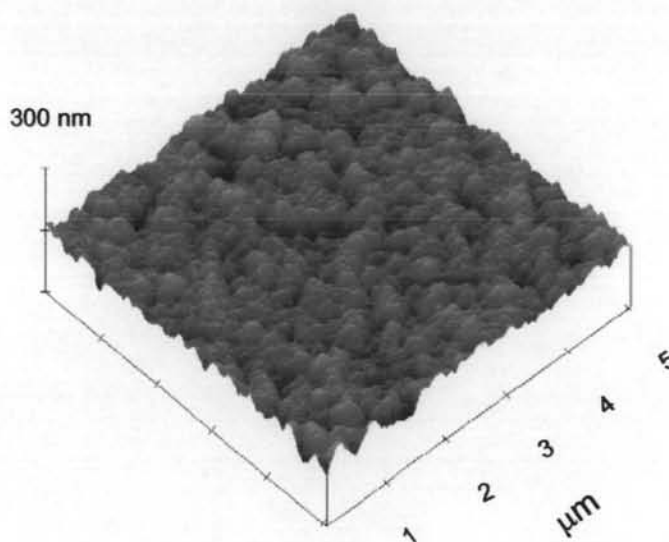


Figure 5.8: (a) SEM photograph, and (b) 3D AFM image of sample VF3, which was grown under the CH_4 of 2.0%, deposition pressure of 30 Torr.

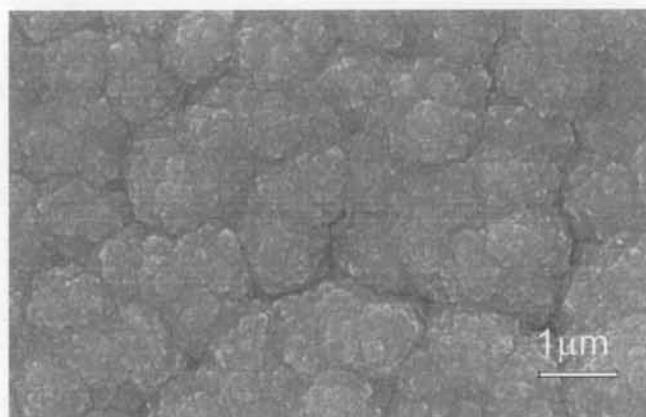


(a)

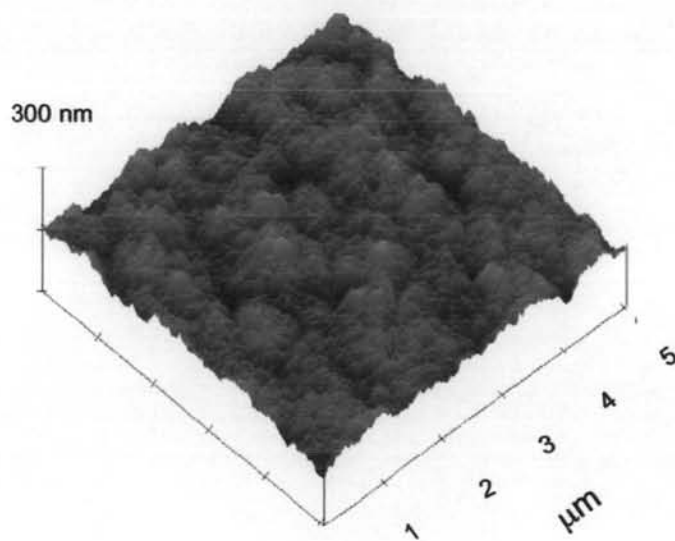


(b)

Figure 5.9: (a) SEM photograph, and (b) 3D AFM image of sample VF4, which was grown under the CH_4 of 3.0%, deposition pressure of 30 Torr.



(a)



(b)

Figure 5.10: (a) SEM photograph, and (b) 3D AFM image of sample VF5, which was grown under the CH_4 of 5.0%, deposition pressure of 30 Torr.

Fig. 5.11 shows the change of grain size and surface roughness at different CH_4 concentrations. At CH_4 concentration of 0.5%, the film shows scattered crystals diamond granule with well-faceted (Fig. 5.6a). The average crystallite size determined by AFM technique is approximately 700 nm. However, in this condition, we do not observe the continuous film on Si substrate. This could be the result from the very low flow rate of CH_4 (0.5 sccm) during growth process.

At higher CH_4 concentration of 1%, the continuous well-faceted film with an average grain size of 353 nm and RMS roughness of 57.3 nm are observed (Fig. 5.7a). We also observed very small grains or secondary diamond nuclei scatter among the large grain boundaries.

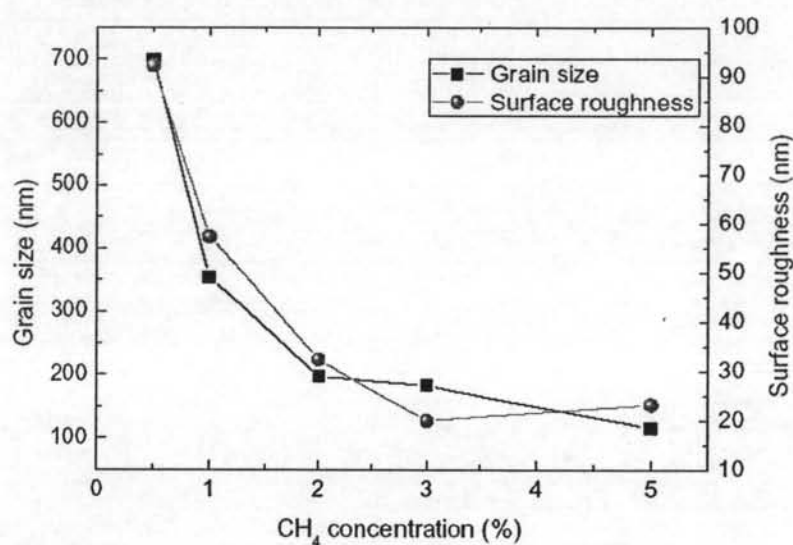


Figure 5.11: Evolution of grain size and surface roughness versus CH_4 concentration.

At higher CH_4 concentration of 2% and 3%, in contrast to the result of film grown at CH_4 concentration of 0.5% and 1%, the surface morphology change to non-faceted films (Fig. 5.8-Fig. 5.9). In these higher CH_4 conditions, the films consist of a small grain particles with an average size of 197 nm and 183 nm, and RMS roughness of 32.3 nm and 19.9 nm for CH_4 concentration at 2% and 3%, respectively.

When increase CH_4 concentration up to 5 %, the surface morphology change to cauliflower-like type (Fig. 5.10). The film consists of groups of cluster with approximately $1.5 \mu\text{m}$ in diameter. Each of clusters also consist of very small grains with average grain size of 116 nm. However, the RMS roughness has increased to 23.2 nm. This could be the result of high number of the groove between each of clusters.

The observation results of film morphology with increased CH_4 concentrations show similar trend to the results of Mallika and Komanduri [28] and Haubner and Lux [51]. Mallika and Komanduri described that with increased CH_4 concentration in the gas phase, the increase in the secondary nucleation on the diamond film and decrease the average grain size could be observed. Haubner and Lux showed that the surface morphology and characteristic of Raman spectrum could be changed with the plasma intensity (surface temperature, atomic hydrogen, and gas pressure) and methane concentration, as showed in Fig. 5.12.

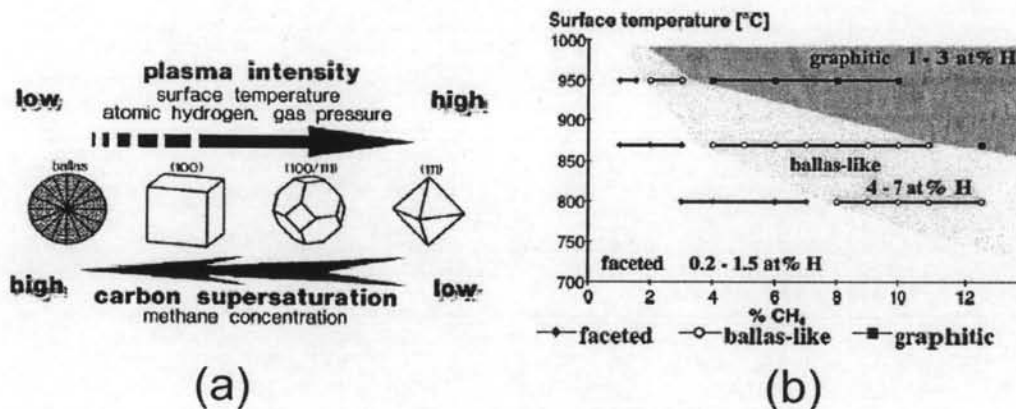


Figure 5.12: The schematic drawing on the morphological changes (a), and the surface morphology changes with surface temperature and CH_4 concentration (b) [51].

With increasing of hydrocarbon or methane concentration, the facets geometry change from (111) to (100) to (100/111), and to ballas shape, as showed in Fig. 5.12a. Moreover, in their experimental results, the faceted diamonds are

usually observed at the surfaced temperature around 800 °C, with decreasing of substrate temperature, the domain boundaries extend to higher methane concentrations in the gas phases, as showed in Fig. 5.12b. As mentioned that our reactor no extra heater was utilized during the deposition process, we do not study the effect of substrate temperature on facets of films. However, in our opinion, it is difficult to determine the exact transition temperature between faceted and ballas surface morphologies this is due to the specific reactor configuration, technology, and many diamond growth parameters. In our results, we showed only the surface morphologies changed with increased CH₄ concentrations.

The decrease of grain size reduces diamond crystallinity. These results will be further discussed in section 5.3.2.

5.3.2 Films qualities

Fig. 5.13 shows Raman spectrum of CVD diamond film grown at CH₄ concentration of 1%, and deposition pressure of 50 Torr, taken with 810 nm and 514.5 nm laser sources.

For films grown at same condition, the Raman spectrum taken with 810 nm laser shows a broad band around 1300 cm⁻¹ and a characteristic diamond peak does not appear. Moreover, the non-diamond phases located around 1550 cm⁻¹ is also undistinguishable. On the contrary, when investigated this film with 514.5 nm laser. The characteristic diamond peak located around 1332 cm⁻¹ and a broad band around 1550 cm⁻¹ can be observed. These observations agree with the results of Leeds et al. [49] and Sun et al. [52]. They studied the effect of different wavelength of laser Raman (240-780 nm) to CVD diamond films investigation. They described that the observed Raman spectrum not only depends on the growth condition of films but also the wavelength of laser being used. Moreover, they found that the Raman spectrum excited at 780 nm (IR laser) is difficult to indicate the peak position, unlike excited at 244 nm (UV laser), this could be due to the absorption or resonance effect. The absorption effect is due

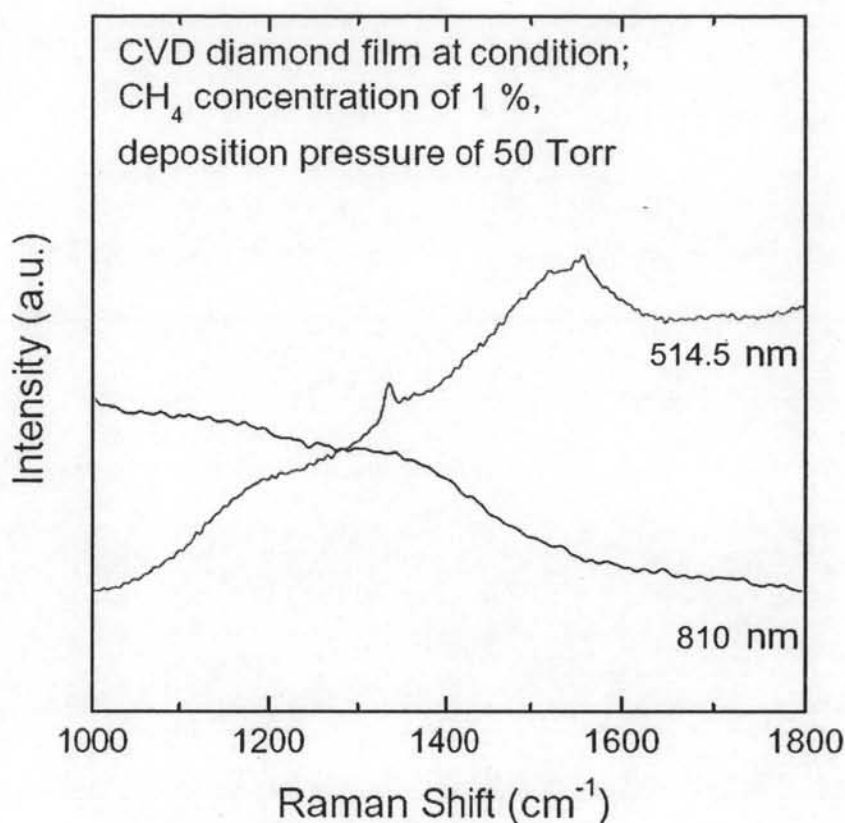


Figure 5.13: Raman spectrum of CVD diamond film, taken by PERKIN ELMER/Spectrum GX NIR FT-Raman laser wavelength of 810 nm (photon energy of 1.53 eV) and 514.5 nm (photon energy of 2.41 eV).

to the differing absorption depth of graphite therefore differing interaction volume at different laser wavelength, it could also be due to a change in the signal intensity [49, 53].

In this work, the argon laser of wavelength 514.5 nm (photon energy of 2.41 eV) is chosen to investigate the bonding in the films.

Raman spectrum of samples VF1-VF5 are compared in Fig. 5.14. For film VF1, which is grown at 0.5% CH₄, the spectrum contains a sharp peak centered at 1333 cm⁻¹ with a FWHM equal to 9.8 cm⁻¹. This is about 5.2 times higher than that of a diamond crystal (calculated from 9.8/1.9). However, the small peak

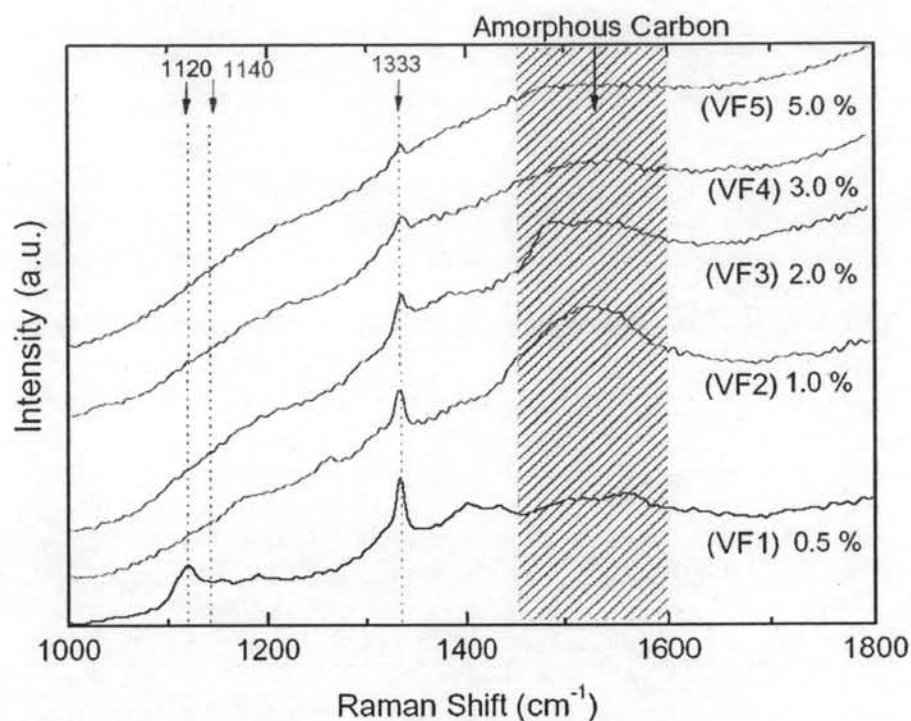


Figure 5.14: Raman spectrum of sample VF1-VF5 using 514.5 nm laser source.

centered at 1120 cm^{-1} is a unknown peak. The broad peak around 1450-1600 cm^{-1} represented as shadow in Fig. 5.14 is amorphous carbon phase. Raman spectrum of sample VF2 is showed in Fig. 5.14(1.0%). It contains a sharp centered at 1333 cm^{-1} with a FWHM equal to 10.2 cm^{-1} , it is about 5.4 times above that of diamond crystal (calculated from 10.2/1.9). In addition, the broad hump peak around 1450-1600 cm^{-1} indicates that film contains amorphous or diamond-like carbon phase, this peak did not appear in the sample VF1.

When increased CH_4 concentration to 2%, 3%, and 5%, a FWHM at 1333 cm^{-1} increase (18.0, 20.0, and 21.0 cm^{-1}) as well as the increase of broad peak around 1450-1600 cm^{-1} , which indicated that film has the lower sp^3 -bond and higher sp^2 -bond. Particulary, at CH_4 concentrations of 3% and 5%, a very broad peak around 1400-1600 cm^{-1} can be observed. We can see that the intensity of Raman peak at 1333 cm^{-1} increased with low FWHM when the CH_4 concentrations decreased, this means that the films have high purity or low defects.

Benndorf et al. [54] showed that the signal intensities of H_{α} (656.3 nm) and H_2 (581.0 nm), which were observed using optical emission spectroscopy (OES) decreased when increased CH_4 concentrations. It should be noted that the high concentration of H_2 is believed to etch graphite phase during diamond growth, as early mentioned. This assumption should be studied in our reactor.

The defects of the polycrystalline diamond film, which are graphite and amorphous phases (χ_{def}) for CH_4 and H_2 gas mixture are given by Equation (5.1)[55],

$$\chi_{def} \propto \frac{[CH_4]}{[H_2]}. \quad (5.1)$$

Thus, the high quality (low graphite or amorphous phases) CVD diamond film could be deposited with low CH_4/H_2 ratio. In general, there are two different types of Raman spectra observed by analyzing the different types of surface morphology, which are diamond layers with amorphous contents and ballas layer with graphitic contents [51]. When compared our results of Raman spectra and the surface morphology with the results of Haubner et al., our films were the diamond layers with amorphous contents at CH_4 concentration of 0.5 and 1%, respectively. In addition, the decrease of grain size could reduce diamond crystallinity and film changes to diamond-like carbon with the ballas or graphitic morphology. Fig. 5.15 shows the evolution of grain size and FWHM of diamond characteristic peak versus CH_4 concentration.

The summary of roughness, grain size, and FWHM at different CH_4 concentration are showed in Table 5.2.

The surface roughness and grain size decrease as CH_4 concentration is increased. In contrast, FWHM of diamond characteristic peak increased as CH_4 concentration is increased. This results are similarity with Park et al. [56] and Hao et al. [57], respectively.

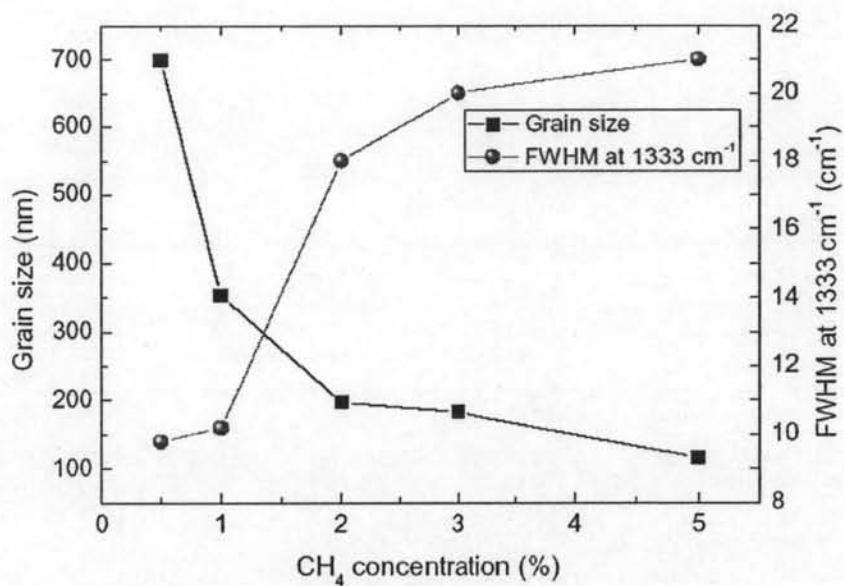


Figure 5.15: Evolution of grain size and FWHM at 1333 cm^{-1} versus CH_4 concentration.

Table 5.2: The roughness, grain sizes, and FWHM (1333 cm^{-1}) of CVD diamond films at different CH_4 concentration.

Sample	Roughness (nm)	Grain size (nm)	FWHM (at 1333 cm^{-1})
(VF1) 0.5% CH_4	92.2	700	9.8
(VF2) 1% CH_4	57.3	353	10.2
(VF3) 2% CH_4	32.3	197	18.0
(VF4) 3% CH_4	19.9	183	20.0
(VF4) 5% CH_4	23.2	116	21.0

5.4 Effect of Deposition Pressures on Diamond Films

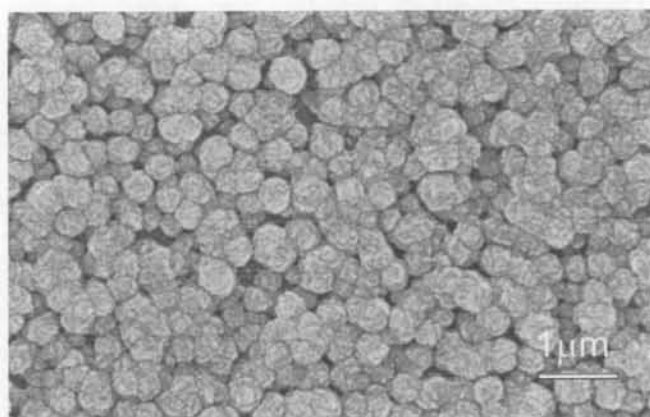
CVD diamond films were deposited under different deposition pressure, as showed in Table 5.3. Samples VP1-VP4 are grown with the microwave power of 450 watt, substrate temperature of 370-470 °C, deposition time of 30 hour, and CH₄ concentration of 1%. The effect of deposition pressure on surface morphology, surface roughness, and the Raman characteristics in the films will be presented and discussed in the following sections.

Table 5.3: Deposition pressures of samples VP1-VP5

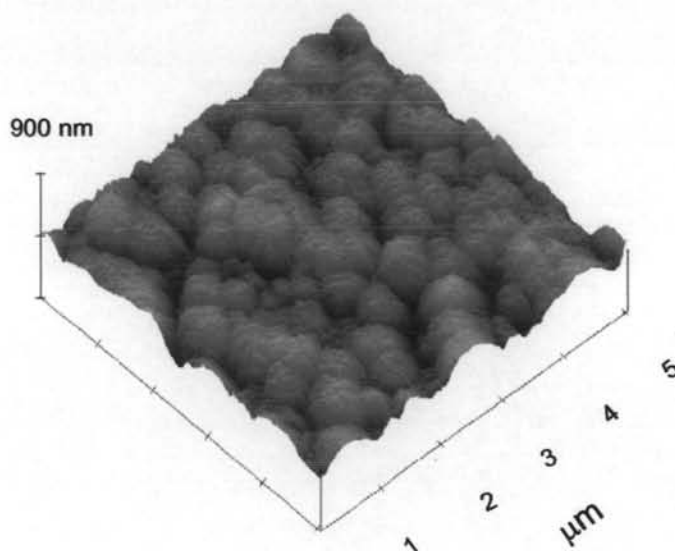
Sample	VP1	VP2	VP3	VP4
Deposition pressure (Torr)	10	30	40	50

5.4.1 Films morphology and roughness

The surface morphology of CVD diamond films taken with SEM and AFM at increased deposition pressure are showed in Fig. 5.16-5.19.

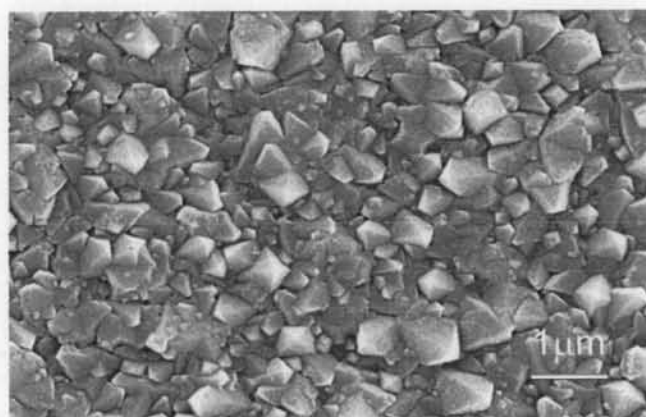


(a)

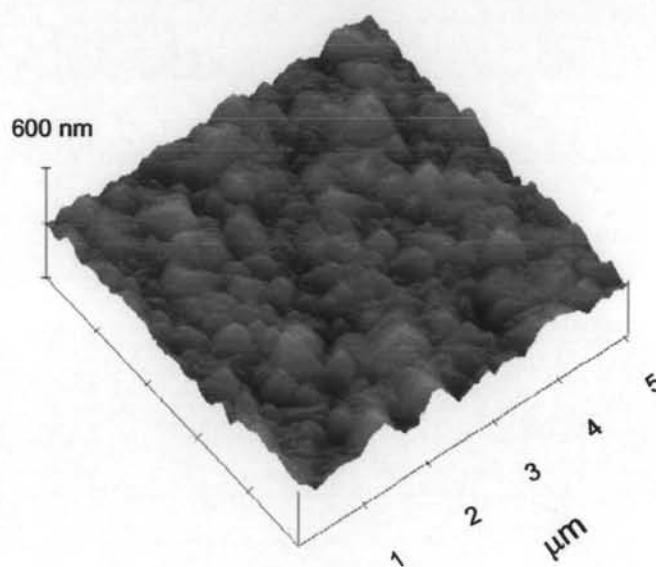


(b)

Figure 5.16: (a) SEM photograph, and (b) 3D AFM image of sample VP1, which was grown under the CH_4 of 1%, deposition pressure of 10 Torr.

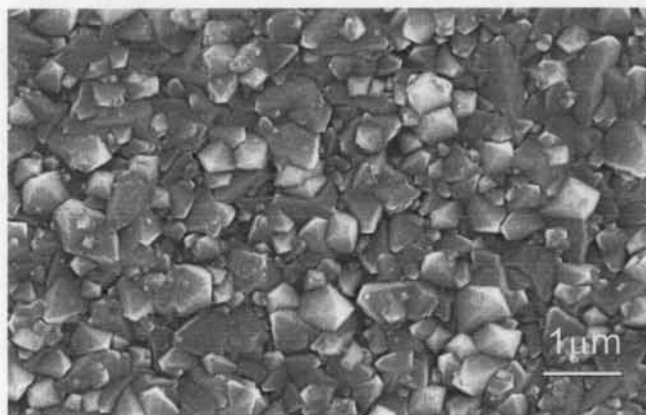


(a)

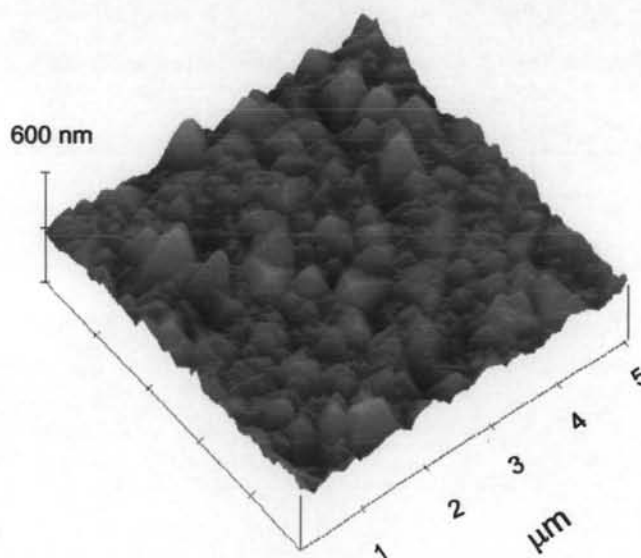


(b)

Figure 5.17: (a) SEM photograph, and (b) 3D AFM image of sample VP2, which was grown under the CH_4 of 1%, deposition pressure of 30 Torr.

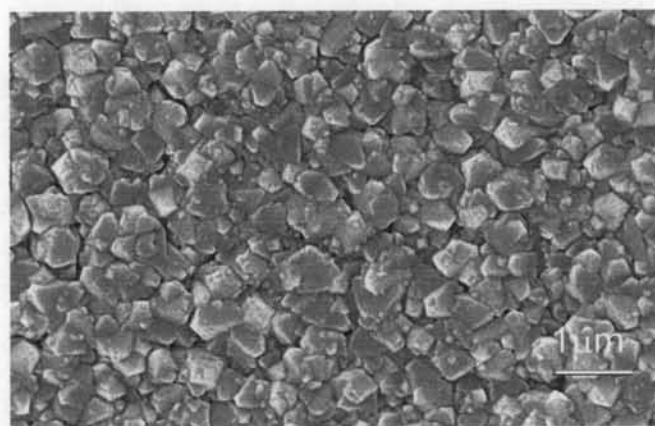


(a)

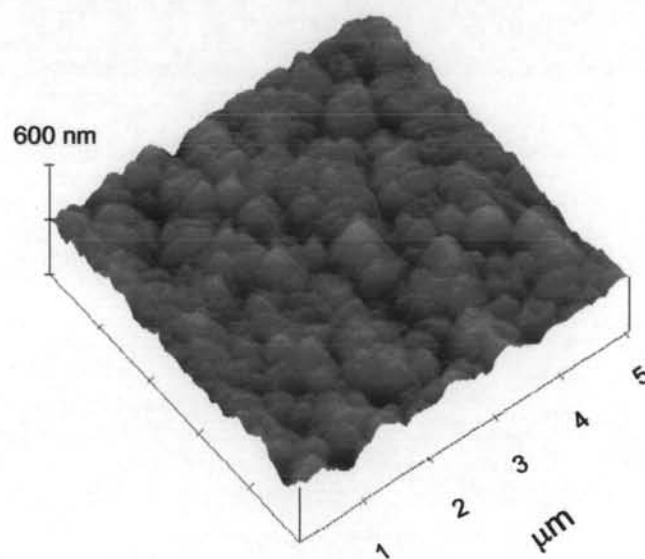


(b)

Figure 5.18: (a) SEM photograph, and (b) 3D AFM image of sample VP3, which was grown under the CH_4 of 1%, deposition pressure of 40 Torr.



(a)



(b)

Figure 5.19: (a) SEM photograph and (b) 3D AFM image of sample VP4, which was grown under the CH_4 of 1%, deposition pressure of 50 Torr.

At deposition pressure of 10 Torr, the surface morphology of film tend to be cauliflower type. The spherical shape with an average grain size of 685 nm and RMS roughness of 83 nm are observed (Fig. 5.16).

With increasing deposition pressure to 30, and 40 Torr, the morphologies of films turn to well-faceted appearance with an average grain size of 353 and 343 nm, respectively. However, for both conditions, abundant of nano-size secondary diamond nuclei deposited between the grain boundaries are observed (Fig. 5.17a, 5.18a). The RMS roughness recorded at 57.3 nm and 59.4 nm for film grown at 30 and 40 Torr, respectively. At higher deposition pressure up to 50 Torr, the amount of secondary nucleation decreases. The average grain size has increased to 400 nm with the RMS roughness of 54.2 nm (Fig. 5.19).

5.4.2 Films qualities

Raman spectrum of samples VP1-VP4 are compared in Fig. 5.20. The Raman spectrum of sample VP1, which is grown at 10 Torr, contains a broad peak around $1300\text{-}1600\text{ cm}^{-1}$. No characteristic peak of diamond were presented, which indicated that the film is lack of diamond crystallinity.

With increasing deposition pressure to 30, 40, and 50 Torr, Raman spectrum of the films contain sharp peaks centered around 1333 cm^{-1} with FWHM in the range of $10.2\text{-}12.0\text{ cm}^{-1}$, it is 5.4-6.3 times higher than that of diamond crystal (calculated from $10.2/1.9\text{-}12.0/1.9$). Additionally, the broad hump around $1450\text{-}1600\text{ cm}^{-1}$ (shadow in Fig. 5.20) can also be observed in sample VP2, VP3, and VP4. This indicated that films also high sp^2 -compound. There are many researchers studied the effect of deposition pressure on CVD diamond film.

Work by Mallika and Komandurri [28], which studied the diamond coated on Si_3N_4 cutting tools, described that at higher pressure, the mean free path between electrons and molecules decreased and hence increased the collision frequency. Therefore, the number of electrons in plasma discharge increases with increased deposition pressure. As a result, the enhancement in the rate of atomic hydrogen

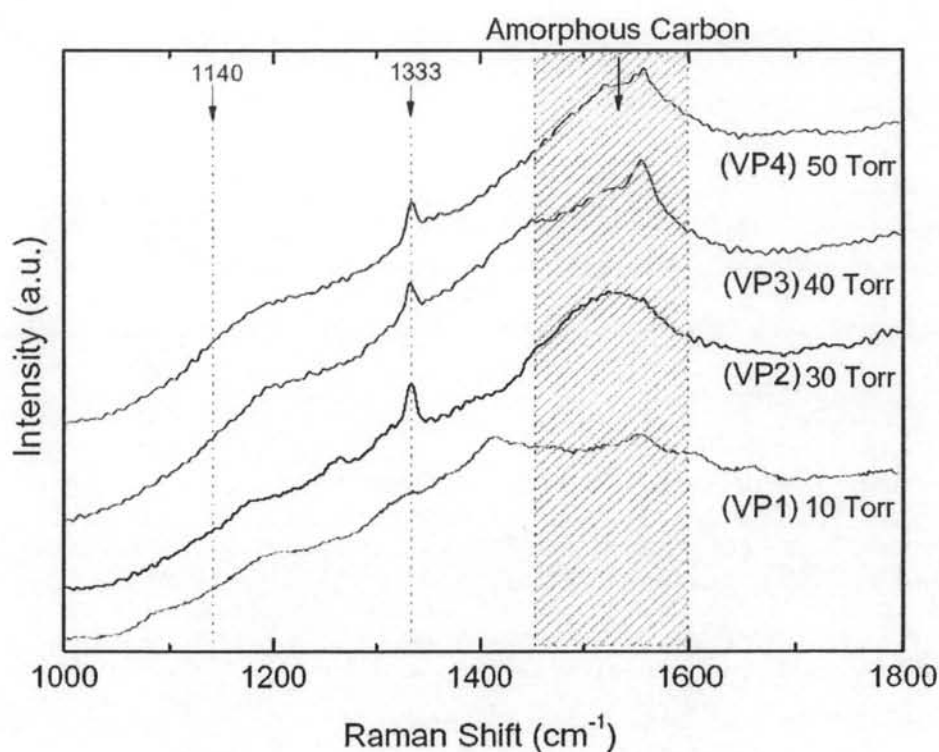


Figure 5.20: Raman spectrum of sample VP1-VP4 using 514.5 nm laser source.

can be achieved which also prevents the non diamond phase to form during growth processes.

In the work by Li et al. [38] showed two distinct morphologies which corroborated with the results from the Raman spectra, diamond layers with amorphous contents and ballas layers with graphitic contents. At a fixed CH₄ concentration of 5 %, with higher pressure of 100, and 125 Torr, the films showed well-faceted diamond morphology with facets larger than 1 μm . In contrast, film grown at low pressure (50, and 75 Torr) yielded only graphitic-flakes. In addition, they also showed that the film growth rate was exponential with increasing pressure. They described that this may not be expected since plasma density increase or decrease with deposition pressure, which changed the arrival rate of radicals at the growth surface. But it may have promoted the formation of carbon dimers in the gas phase, which were the precursors for diamond growth.

Asmussen and Reinhard [55] described that for H_2 at low pressure (<few tens of Torr), plasma has low temperature and the electrons impaction dissociation can be dominant characteristic. Thus, CH_4 chemical reactions are difficult to converse to CH_3 and C_2H_2 radicals, which are important for diamond growth processes.

Potocky et al. [58] showed that at high substrate temperature (≥ 600 °C), the Raman spectrum of the film displayed one dominant peak located at 1333 cm^{-1} that confirmed presence of diamond. While, at low substrate (≤ 400 °C), the non-diamond phases increased.

However, in our opinion, the low diamond crystallinity at 10 Torr, could be due to the low substrate temperature (370-430 °C) during growth processes. It should be noted that in our experiment, no extra heater was utilized during the deposition processes. Thus, the samples were only heated by the microwave plasma. The summary of roughness, grain size, and FWHM at different deposition pressure are showed in Table 5.4.

Table 5.4: The roughness, grain sizes, and FWHM (1333 cm^{-1}) of CVD diamond films at different CH_4 concentration and deposition pressure.

Sample	Roughness (nm)	Grain size (nm)	FWHM (at 1333 cm^{-1})
(VP1) 10 Torr	83.0	685	not found
(VP2) 30 Torr	57.3	353	10.2
(VP2) 40 Torr	59.4	343	11.8
(VP2) 50 Torr	54.2	400	11.8